JOURNAL OF SPACECRAFT AND ROCKETS
Vol. 29, No. 6, November–December 1992

Parametric Study of Manned Aerocapture Part I: Earth Return from Mars

J. Evans Lyne*
Eloret Institute, Palo Alto, California 94303
M. E. Tauber†
NASA Ames Research Center, Moffett Field, California 94035
and
Robert D. Braun‡
NASA Langley Research Center, Hampton, Virginia 23665

A parametric study of the Earth return aerocapture for a manned Mars mission is described. The variation of entry corridor width and stagnation-point heating with vehicle arrival velocity, lift-to-drag ratio (L/D), and ballistic coefficient (m/C_DA) are examined. To maximize corridor widths, the aerocapture maneuvers employ variable bank-angle trajectories. Vehicles with an L/D of 0.5 or more are found to provide a corridor width of at least 0.7 deg while keeping the peak deceleration load below 5 g for approach velocities up to 14.5 km/s. Vehicle convective heating calculations are performed assuming a fully catalytic "cold" wall; radiative heating is computed assuming that the shock layer is in thermochemical equilibrium. As expected, heating rates are great enough to require ablative thermal protection systems in all cases. Stagnation-point peak heating rates and integrated heat load are shown to depend critically on both entry velocity and ballistic coefficient. For the most severe cases considered, peak heating and integrated heat load are several times greater than those encountered by Apollo but within the range of experience for unmanned vehicles.

Nomenclature

A	= entry vehicle reference area, m^2
C_D	= entry vehicle drag coefficient
D	= drag, N
L	= lift, N
m	= mass, kg
m/C_DA	= ballistic coefficient, kg/m^2
R_n	= nose radius, m
V_e	= velocity at atmospheric interface, km/s
α	= angle of attack

Introduction

MANNED Mars missions have been extensively studied during the last 30 years. These investigations have shown repeatedly that the use of atmospheric drag rather than propulsion to slow the spacecraft upon arrival at Mars or Earth could result in large savings in the initial weight required in low Earth orbit (LEO).[1,2] For an aerocapture to be successful, the vehicle must dissipate enough energy in its initial pass through the atmosphere to be captured into a planetocentric orbit without overheating or subjecting the crew and structure to excessive deceleration. To accomplish this, the vehicle's entry angle must fall within a fairly narrow range known as the entry corridor. If the angle is too small, the vehicle will fail to be captured and continue in a heliocentric orbit; conversely, if the entry angle is too steep, the vehicle will either hit the surface, overheat, or subject the crew and structure to excessive deceleration loads[3] (Fig. 1). The location and width of the entry corridor depend on the vehicle's arrival velocity V_e and aerodynamic characteristics, namely, the ballistic coefficient m/C_DA and lift-to-drag ratio, L/D. For certain entry conditions and vehicle configurations, no atmospheric trajectory can be flown which will capture the vehicle into a satisfactory orbit without exceeding an imposed deceleration load limit (that is, no entry corridor exists).

Current proposals for manned Mars missions differ significantly with respect to the Earth return conditions.[4] Some scenarios involve conjunction class interplanetary transfers which result in Earth arrival velocities of 11.5–12 km/s and require round-trip times of approximately 3 yr. Other concepts employ opposition class missions which permit shorter trip durations but result in Earth arrival velocities of approx-

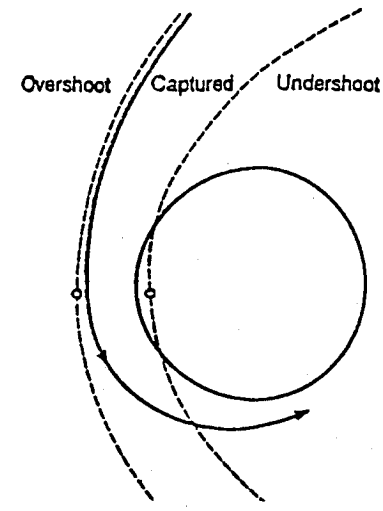

Fig. 1 Entry corridor.

Received July 2, 1991; presented as Paper 91-2874 at the Atmospheric Flight Mechanics Conference, New Orleans, LA, Aug. 12–14, 1991; revision received April 13, 1992; accepted for publication April 24, 1992. This paper is declared a work of the U.S. Government and is not subject to copyright protection in the United States.

*Research Scientist, Thermosciences Division, NASA Ames Research Center. Student Member AIAA.

†Senior Research Scientist, Thermosciences Division. Associate Fellow AIAA.

‡Aerospace Engineer, Space Systems Division. Member AIAA.

Table 1 Range of parameters

Ballistic coefficient, kg/m^2	50, 100, 300, and 500
Vehicle maximum L/D	0.2, 0.3, 0.5
Vehicle entry velocity, km/s	11.5, 12.0, 13.0, and 15.0

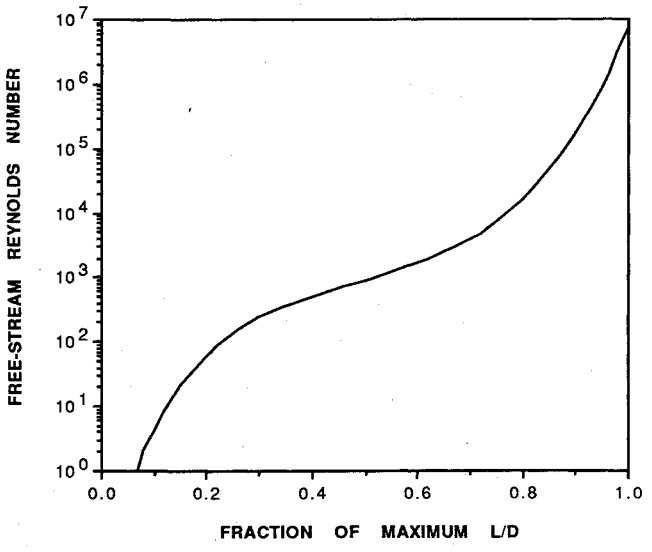

Fig. 2 Decrease of vehicle L/D with Reynolds number.

imately 13–15 km/s. In general, as arrival velocity increases, the control authority (L/D) required for a successful aerocapture also increases. Since packaging is more complex for high L/D configurations,[5] the required level of control authority is an important determinant of mission architecture. Another factor influencing mission planning is aerodynamic heating and its effect on vehicle weight and design. Heating rate primarily influences the type of material required for the thermal protection system (TPS). For example, radiative cooling using ceramic tiles similar to those on the Space Shuttle is appropriate only for rates up to about 25 W/cm^2. For single-use applications, carbon-carbon materials with antioxidation coatings can withstand approximately 100 W/cm^2. At higher heating rates, radiative cooling is not feasible, and ablative shields become necessary. Heat load determines the weight of the TPS by governing the thickness of insulation and/or ablator required. Both heating rate and integrated load vary significantly over the range of potential Earth entry conditions. Therefore, the objective of this study was to examine L/D requirements and stagnation-point heating for a spectrum of probable entry conditions and vehicle configurations (Table 1).

Study Parameters

Trajectory Constraints

Throughout this investigation, all aerocapture trajectories were required to meet several constraints. First, the maneuver had to result in a low Earth orbit with a period of approximately 90 min. (For a few cases, periods up to 166 min were allowed.) The rationale for choosing low Earth orbits was to facilitate rendezvous with the Shuttle or space station and to avoid the hazards of the Van Allen radiation belts. In addition, the peak load factor on the vehicle and crew was not allowed to exceed 5 g. This constraint was set to avoid overstressing the crew members who will be physiologically deconditioned after many months of weightlessness. The choice of a 5-g limit is supported by Soviet experience with 5-g entries upon return from the Mir space station after flights in excess of 8 months.[6] The vehicle is also required not to pass below an altitude of 55 km at any point in its trajectory. This constraint is designed to indirectly limit peak heating levels. Lastly, attempts have been made to limit entry vehicle roll rates to approximately 12 deg/s, although this has not been an absolute requirement.

Atmospheric Model

The atmospheric density model that was used simulated the density profile of the 1976 U. S. Standard Atmosphere with a series of exponential expressions. The entry interface was set at 122 km (400,000 ft), and the atmosphere was assumed to be nonrotating and not varying with latitude, longitude, or season. An empirical correlation was used to decrease the peak vehicle L/D at high altitudes to account for increased laminar skin friction relative to wave drag in this flight regime (Fig. 2). This correlation was developed by plotting calculated and measured lift-to-drag ratios at various Reynolds numbers as a fraction of the high Reynolds number L/D for several vehicles; Fig. 2 represents an approximate curvefit to these points. The data used were from direct simulation Monte Carlo (DSMC) computations for the Space Shuttle[7] and the Aeroassist Flight Experiment vehicle,[8] Apollo and Gemini capsule wind-tunnel tests,[9,10] and X-20A hot-shot wind-tunnel tests.[11]

Trajectory and Heating Calculations

The flight of an unpowered vehicle in a nonrotating atmosphere is described by a system of four first-order, ordinary differential equations.[12] These equations were solved numerically by two iterative computer algorithms. The first of these found a satisfactory trajectory near the overshoot limit; for this case, the vehicle was flown lifting fully downward (bank angle of 180 deg) and complete trajectories were calculated for entry angles which were increased in discrete steps until the vehicle was captured into the desired orbit. The second algorithm found a satisfactory trajectory at the undershoot limit. To do this, the vehicle was initially flown lifting fully upward and, in sequential trajectory calculations, the entry angle was gradually increased until the peak load reached 5 g. At this point, the undershoot boundary had been found; using this value as the entry angle, the algorithm then systematically varied the vehicle roll angle just prior to and after the time of peak deceleration until the final orbital period fell into the desired range. The use of a variable bank angle allows steeper

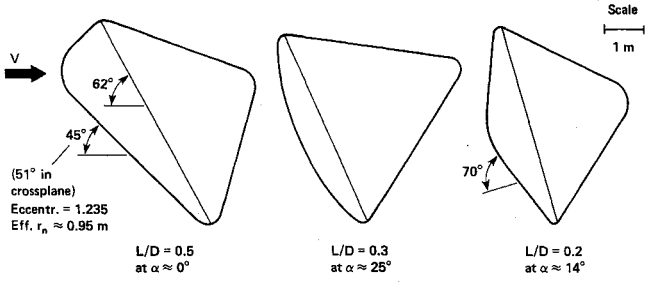

Fig. 3 Entry configurations considered.

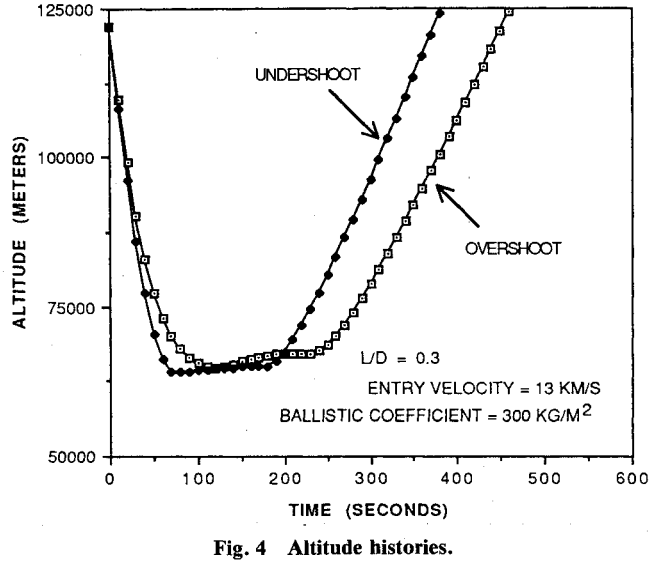

Fig. 4 Altitude histories.

undershoot limits (and thus wider entry corridors) than are possible with the fixed bank angle trajectories employed in many previous studies.[5,13,14] A variable bank-angle scheme similar to the one used here was recently described by Braun and Powell[15]; preliminary comparisons have shown these two algorithms to yield very similar results.

Stagnation-point heating rate and integrated heat load were calculated using the methods described in Refs. 16 and 17. Both convective and equilibrium radiative processes were considered. Only the "cold" wall heating rates occurring in the absence of ablation have been calculated. The results presented are, therefore, independent of the heat shield material and can be used for a variety of candidate materials. All calculations were made assuming that the inviscid shock layer was in thermochemical equilibrium.

The technique for calculating stagnation-point radiative heating given in Ref. 17 is a simple correlation expression which is applicable for vehicles with nose radii of 1.0–3.0 m flying at speeds between 10 and 16 km/s and at altitudes of 54–72 km (the altitude regime in which the vast majority of radiative heating occurs at Earth). This expression gives the heating rate as a function of nose radius, local atmospheric density, and vehicle velocity. The correlation is based on calculations that used a multiband radiation model which accounts for self-absorption and the nonadiabatic nature of the flow. Ref. 17 compares the results of this technique with those of other computational methods and found maximum discrepancies of 20–30%. Uncertainties of this magnitude are quite common in radiative heating calculations and are not considered unacceptably high for the purposes of this study.

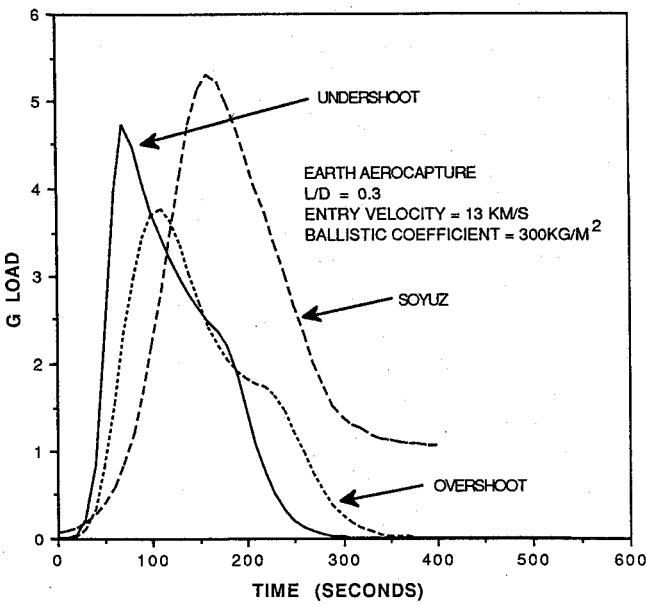

Fig. 5 Typical aerocapture g loads compared to Soyuz entry.

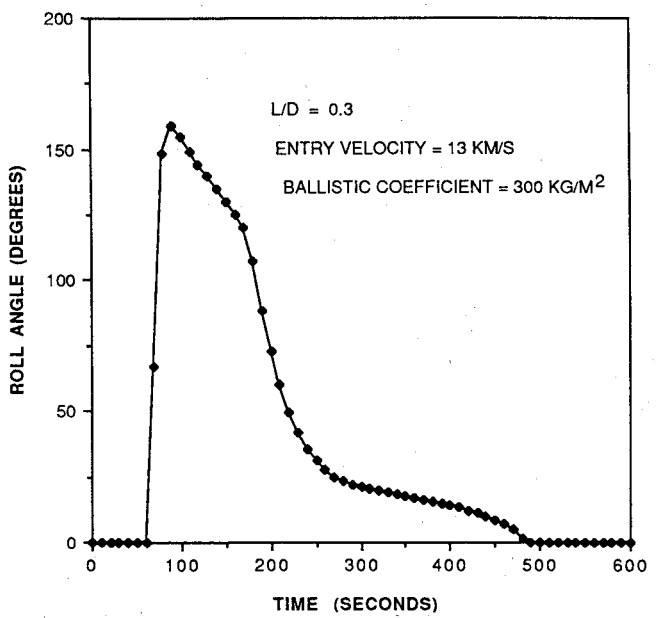

Fig. 6 Vehicle roll-angle history.

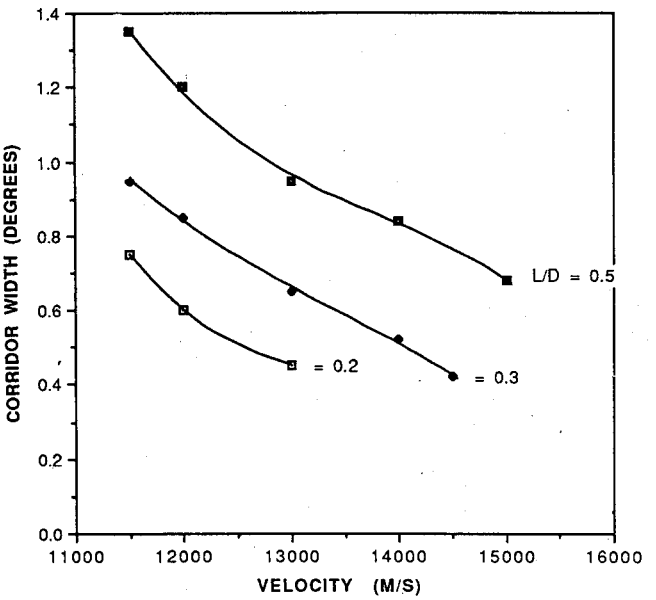

Fig. 7 Corridor width vs entry-velocity (ballistic coefficient = 300 kg/m²).

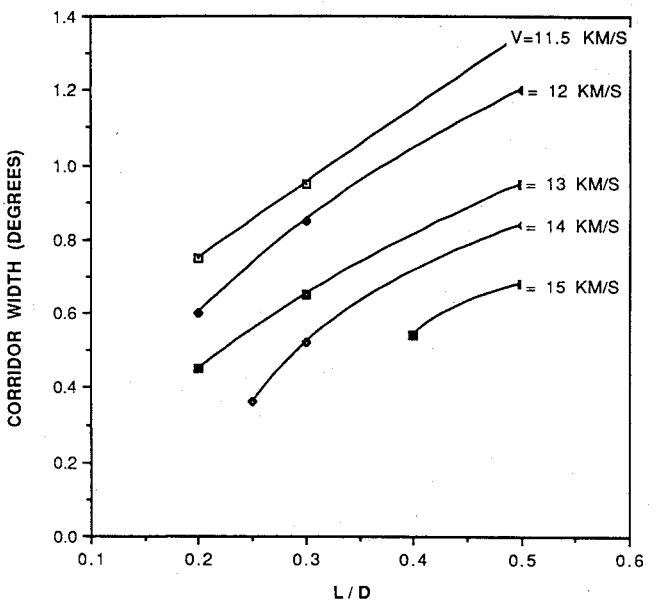

Fig. 8 Corridor width vs L/D (ballistic coefficient = 300 kg/m²).

Entry Vehicles

The vehicle configurations[18] considered are shown in Fig. 3. The capsule on the right is a blunted, 70-deg half-angle cone similar to the Viking probe which landed on Mars in 1976. The center vehicle is identical in shape to the Apollo command module, while the configuration at left is a blunted, raked cone with a slightly elliptical cross section. As indicated in the figure, the vehicles' L/D ranged from 0.2 to 0.5. The first two shapes were chosen to utilize the existing technology base. The capsules were sized to avoid the need for on-orbit assembly while providing adequate room for the crew and specimens. Using as small an entry vehicle as feasible will minimize weight and decrease radiative heating by avoiding large nose radii and thick shock layers. In general, low ballistic coefficients are

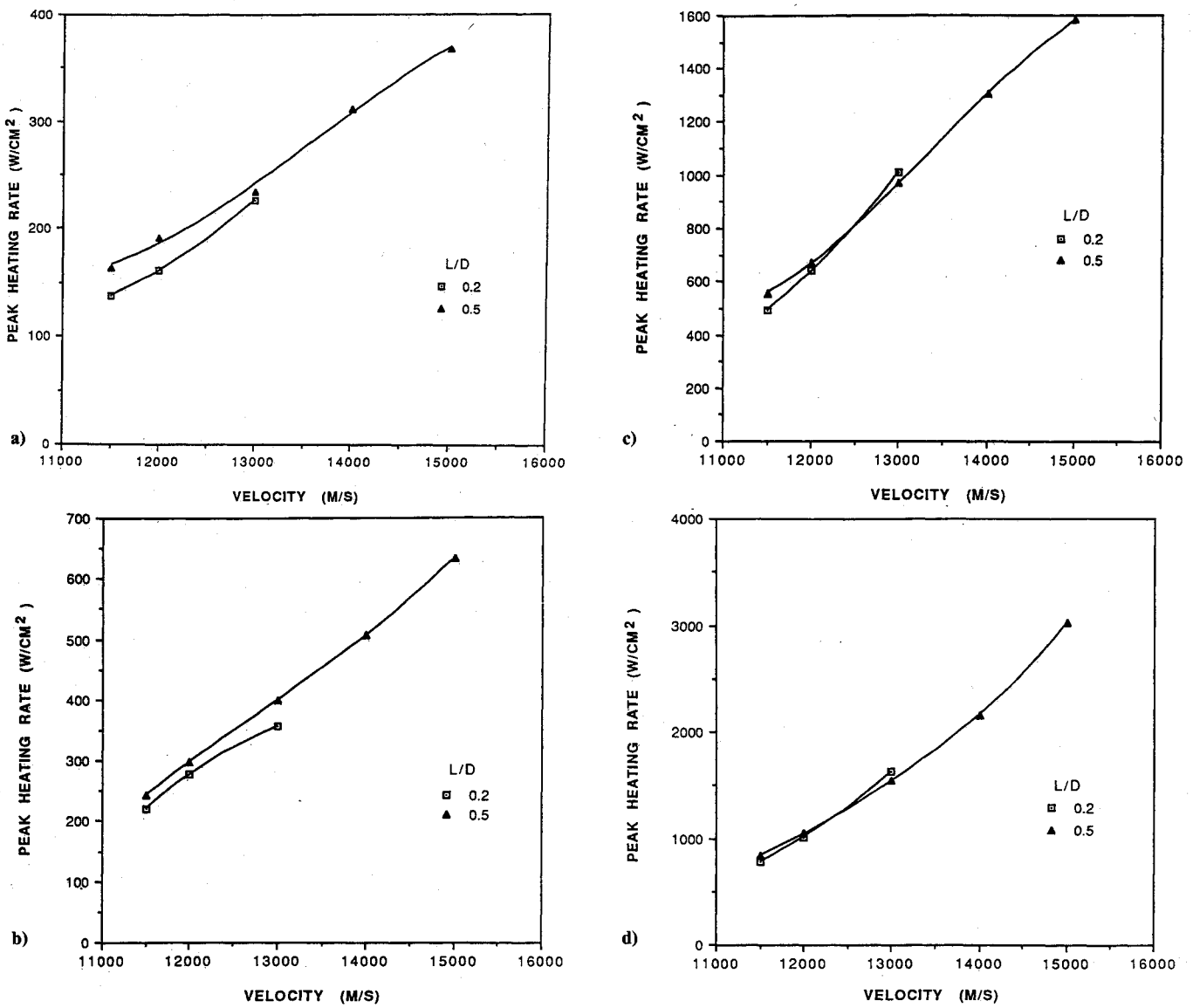

Fig. 9 Undershoot trajectory peak stagnation-point heating rate: a) ballistic coefficient = 50 KG/M^2; b) ballistic coefficient = 100 KG/M^2; c) ballistic coefficient = 300 KG/M^2; d) ballistic coefficient = 500 KG/M^2.

desirable since they result in deceleration at high altitude and thus relatively benign heating environments. However, entries were calculated for a range of m/C_DA from 50 to 500 kg/m^2. The nose radii used for stagnation-point heating calculations are indicated in Fig. 3.

Results

Typical entry trajectories for undershoot and overshoot cases are shown in Fig. 4. The corresponding deceleration pulses are shown in Fig. 5 and compared to that for the entry of a Soyuz capsule on return from the Mir space station. The Soyuz entry was calculated using an L/D of 0.13 and a ballistic coefficient of 600 kg/m^2 (derived from data in Ref. 19). The calculated trajectory assumed entry from a decaying orbit, and the peak g load matched that described by Cosmonaut Atkov. The vehicle bank-angle history used to achieve the undershoot trajectory for this particular aerocapture is illustrated in Fig. 6.

Corridor width is shown as a function of entry velocity for a ballistic coefficient of 300 kg/m^2 in Fig. 7. (These curves varied little either qualitatively or quantitatively for the other ballistic coefficients studied.) For each case, the undershoot boundary was determined by the 5-g limit. This is in sharp contrast to Martian entry studies, which show the undershoot boundary to be set by the energy requirements of the target orbit for many low entry velocity cases.[20] Corridor width is

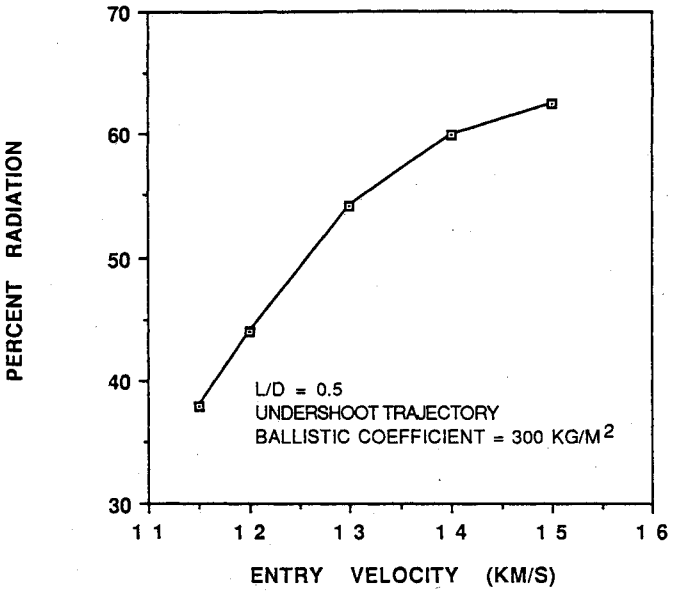

Fig. 10 Percent of peak heating due to radiation for the Earth return undershoot trajectory.

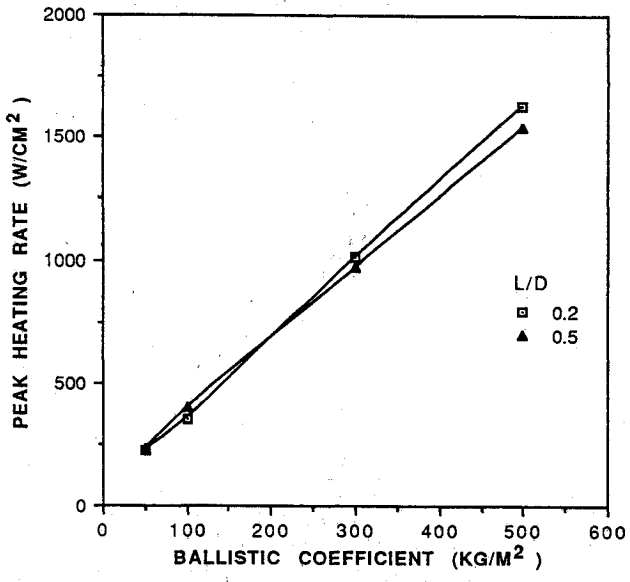

Fig. 11 Undershoot trajectory stagnation-point peak heating rate (entry velocity = 13000 m/s).

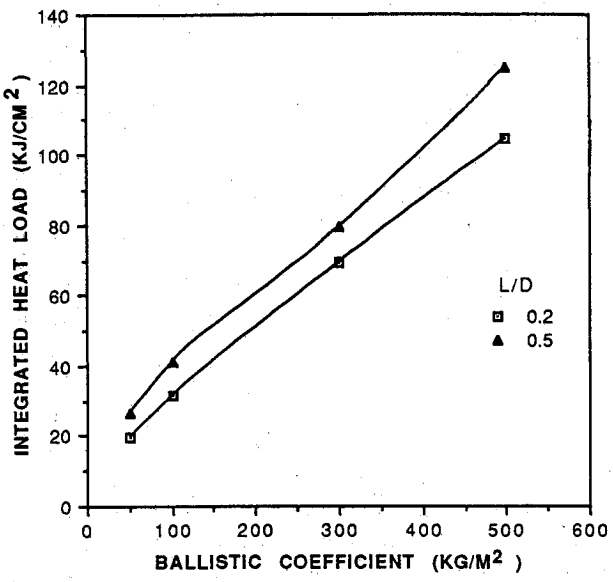

Fig. 12 Overshoot trajectory stagnation-point integrated heat load (entry velocity = 13000 m/s).

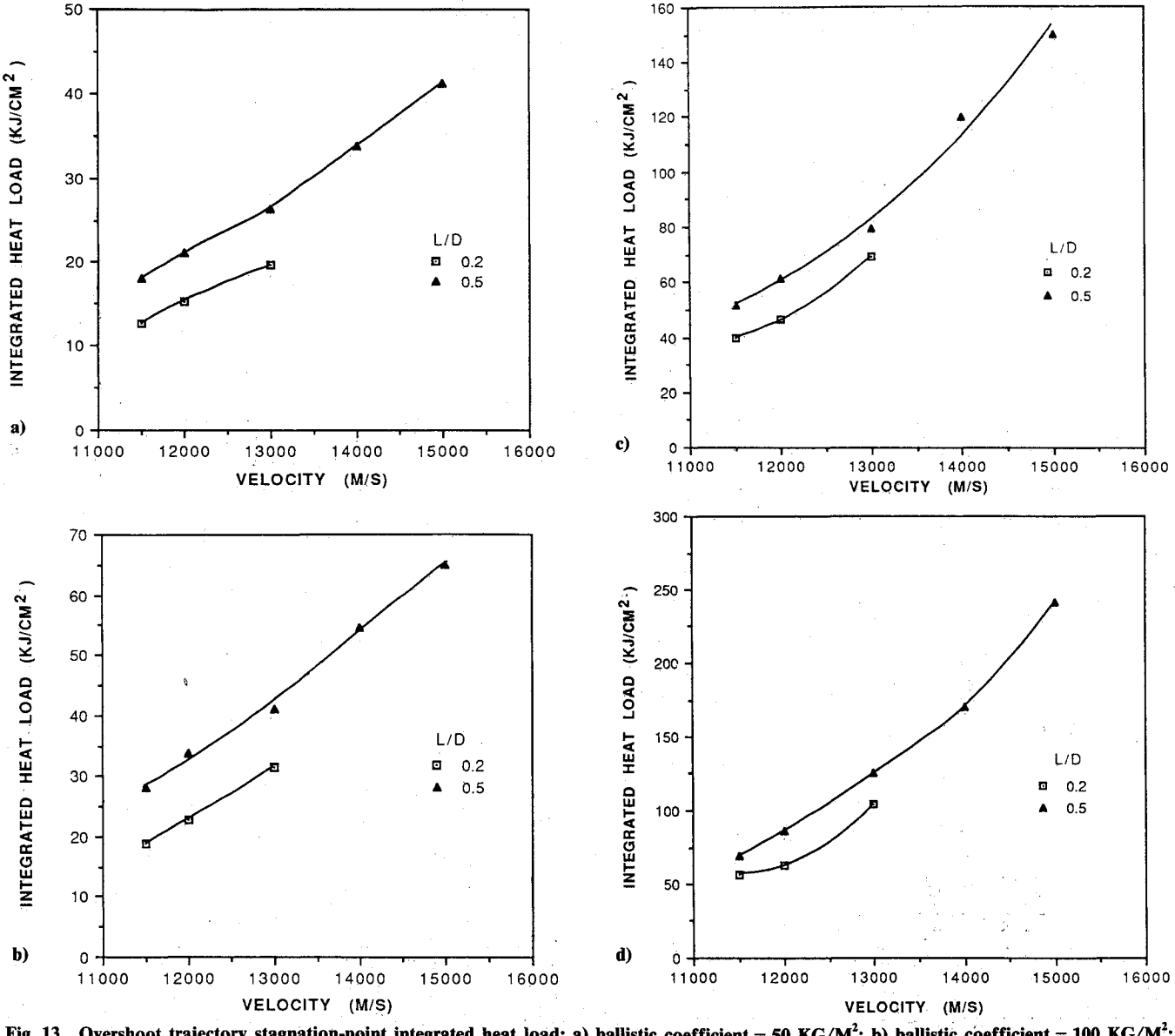

Fig. 13 Overshoot trajectory stagnation-point integrated heat load: a) ballistic coefficient = 50 KG/M^2; b) ballistic coefficient = 100 KG/M^2; c) ballistic coefficient = 300 KG/M^2; d) ballistic coefficient = 500 KG/M^2.

presented as a function of L/D for the various entry speeds in Fig. 8 (m/C_DA = 300 kg/m^2). For the 14-km/s and 15-km/s cases, vehicles with an L/D below those indicated failed to successfully capture.

The entry corridor must be wide enough to allow for inaccuracies in the encounter navigation system as well as atmospheric and aerodynamic dispersions. Recent studies recommend the equivalent of a 0.7-deg corridor width.[21] If this criterion is applied here, the aerobrake is found to require an L/D between 0.4 and 0.5 if entries up to 14.5 km/s are allowed.

Figure 9 shows undershoot trajectory stagnation-point peak heating rates as a function of entry velocity for the range of ballistic coefficients. (Undershoot trajectories are known to experience the highest heating rates whereas overshoot trajectories have the greatest heat loads.) As expected, heating rates increase dramatically with velocity. For the 11.5-km/s entries, peak rates are about the same as those experienced by the Apollo command modules upon return from the Moon (approximately 500 W/cm^2—see Ref. 22). In general, the peak rates are very close to those calculated in Ref. 18 for direct-entry returns from Mars. The most severe cases considered result in a peak heating rate of 2–3 kW/cm^2. Although this is considerably above what has been encountered on previous manned missions, it is an order of magnitude less than the peak rate expected for the Galileo probe during entry at Jupiter.[23] The relative significance of convective and radiative heating vary widely with entry velocity, m/C_DA, and L/D. Radiation accounts for a higher fraction of the total peak heating as both ballistic coefficient and V_e increase (Fig. 10). The pronounced effect of ballistic coefficient on peak heating rate is illustrated in Fig. 11. It is noteworthy that over the range of values considered in this study, ballistic coefficient has a much greater effect on peak heating rate than does entry velocity. Typically, peak heating varies by a factor of 3 between entry velocities of 11.5 and 15 km/s. Conversely, it varies by a factor of 5 to 9 over the range of ballistic coefficients considered. In all cases, the maximum heating was great enough to require the use of ablative heat shields. It should be noted that L/D has little effect on the peak stagnation-point heating rate.

The integrated stagnation-point heat load for overshoot trajectories is shown as a function of ballistic coefficient in Fig. 12 and as a function of entry velocity in Fig. 13. As points of reference, the integrated load for the Apollo 6 command module was 43 kJ/cm^2 (Ref. 22), whereas while that expected for the Galileo probe is approximately 800 kJ/cm2. Although the most severe cases considered here exceed manned flight experience, they are well within the range of unmanned missions. Just as they did for the peak heating rate, ballistic coefficient and entry velocity play the dominant roles in determining the integrated heating load. However, vehicle L/D has a greater effect on integrated load than it did on peak rate, with total heating increasing with L/D. This results from the long duration, shallow, overshoot trajectories which can be achieved by high L/D vehicles, and is particularly prominent for low ballistic coefficient cases where control authority is greatest.

Conclusions

A parametric study of the Earth return aerocapture for a manned Mars mission was conducted. The entry vehicle was captured into a low Earth orbit and was required to observe a peak deceleration limit of 5 g. Variable bank-angle trajectories were used to maximize corridor width. If a corridor width requirement of 0.7 deg is assumed, vehicles with an L/D of 0.4–0.5 are found to be satisfactory for arrival speeds up to 14.5 km/s.

Convective heating calculations were performed assuming a fully catalytic, "cold" wall; radiative heating was computed assuming that the shock layer was in thermochemical equilibrium. Stagnation-point peak heating rate and integrated load were shown to depend critically on ballistic coefficient and entry velocity, while vehicle L/D influences the integrated loads but has little impact on peak rate. Although many of the cases considered result in aerothermal environments more severe than those encountered on previous manned missions, they are well within the range of experience for unmanned vehicles.

Acknowledgments

This research is supported by NASA Grant NAGW-1331 to the Mars Mission Research Center at North Carolina State University.

References

[1]Clark, B., "Manned Mars Missions for the Year 2000," AIAA Paper 89-0512, Jan. 1989.

[2]Menees, G. P., "Aeroassisted Vehicle Design Studies for Manned Mars Missions," International Astronautical Federation/International Academy of Astronautics Paper 87-433, Oct. 1987.

[3]Chapman, D. R., "An Analysis of the Corridor and Guidance Requirements for Supercircular Entry into Planetary Atmospheres," NASA TR R-55, 1959.

[4]Walberg, G. D., "A Review of Aerobraking for Manned Mars Missions," International Astronautical Federation Paper 88-196, Oct. 1988.

[5]Wilcockson, W. H., "L/D Requirements for Manned Mars Aerocapture Missions," AIAA Paper 90-2937, Aug. 1990.

[6]Atkov, O. Y., personal communication, Head, All Union Cardiology Research Center, Moscow, Nov. 29, 1990.

[7]Bird, G. A., "Application of the Direct Simulation Monte Carlo Method to the Full Shuttle Geometry," AIAA Paper 90-1692, June 1990.

[8]Alison, J. F., "Evaluation of an Approximate Technique to Predict Aeroassist Flight Experiment (AFE) Aerodynamics in Hypersonic Transition Regime Flows," Master's Degree Thesis, The Univ. of Alabama at Huntsville, Huntsville, AL, May 1990.

[9]Griffith, B. J., and Boylan, D. E., "Postflight Apollo Command Module Aerodynamic Simulation Tests," *Journal of Spacecraft and Rockets,* Vol. 5, No. 7, 1968, pp. 843–848.

[10]Griffith, B. J., "Comparison of Aerodynamic Data From the Gemini Flights and AEDC-VKF Wind Tunnels," *Journal of Spacecraft and Rockets,* Vol. 4, No. 7, 1967, pp. 919–924.

[11]Performance Group, "Glider Performance Characteristics Report," Boeing Document D2-8080-1, Seattle, WA, Aug. 1963.

[12] Vinh, N. X., Busemann, A., and Culp, R. D., *Hypersonic and Planetary Entry Flight Mechanics,* Univ. of Michigan Press, Ann Arbor, MI, 1980, pp. 100–107.

[13]Braun, R. D., "The Effect of Interplanetary Trajectory Options on a Manned Mars Aerobrake Configuration," NASA TP-3019, July 1990.

[14]Brand, T. J., Fuhry, D. P., and Shepperd, S. W., "An Onboard Navigation System which Fulfills Mars Aerocapture Guidance Requirements," AIAA Paper 89-0629, Jan. 1989.

[15]Braun, R. D., and Powell, R. W., "A Predictor-Corrector Guidance Algorithm for Use in High-Energy Aerobraking Systems Studies," AIAA Paper-91-0058, Jan. 1991.

[16]Marvin, J. G., and Deiwert, G. S., "Convective Heat Transfer in Planetary Gases," NASA TR R-224, July 1965.

[17]Tauber, M. E., and Sutton, K., "Stagnation Point Radiative Heating Relations for Earth and Mars Entries," *Journal of Spacecraft and Rockets,* Vol. 28, No. 1, 1991, pp. 40–42.

[18]Tauber, M. E., Palmer, G. E., and Yang, L., "Earth Atmospheric Entry Studies for Manned Mars Missions," AIAA Paper 90-1699, June 1990.

[19]Wilson, A. (ed.), *Interavia Space Directory,* Interavia, Geneva, 1990, p. 110.

[20]Lyne, J. E., Anagnost, A., and Tauber, M. E., "A Parametric Study of Manned Aerocapture at Mars," AIAA Paper 91-2871, Aug. 1991.

[21]Wilcockson, W. H., "OTV Aeroassist with Low L/D," *Acta Astronautica,* Vol. 17, No. 3, 1988, pp. 277–301.

[22]Curry, D. M., and Stephens, E. W., "Apollo Ablator Thermal Performance at Superorbital Entry Velocities," NASA TN D-5969, Sept. 1970.

[23]Moss, J. N., "A Study of the Aerothermal Entry Environment for the Galileo Probe," AIAA Paper 79-1081, June 1979.

Gerald T. Chrusciel
Associate Editor